



UNIVERSITY OF LEEDS

This is a repository copy of *Use of Two-Pressure-Head Method to Assess Water Permeability of Structural Concrete*.

White Rose Research Online URL for this paper:
<http://eprints.whiterose.ac.uk/129928/>

Version: Accepted Version

Article:

Yang, K, Yang, C, Long, A et al. (1 more author) (2018) Use of Two-Pressure-Head Method to Assess Water Permeability of Structural Concrete. *Materials Journal*, 115 (1). pp. 65-75. ISSN 0889-325X

10.14359/51700992

This article is protected by copyright. All rights reserved. This is an author produced version of a paper published in the *Materials Journal*. Uploaded in accordance with the publisher's self-archiving policy.

Reuse

Items deposited in White Rose Research Online are protected by copyright, with all rights reserved unless indicated otherwise. They may be downloaded and/or printed for private study, or other acts as permitted by national copyright laws. The publisher or other rights holders may allow further reproduction and re-use of the full text version. This is indicated by the licence information on the White Rose Research Online record for the item.

Takedown

If you consider content in White Rose Research Online to be in breach of UK law, please notify us by emailing eprints@whiterose.ac.uk including the URL of the record and the reason for the withdrawal request.



eprints@whiterose.ac.uk
<https://eprints.whiterose.ac.uk/>

USE OF A TWO PRESSURE-HEAD METHOD TO ASSESS THE WATER PERMEABILITY OF STRUCTURAL CONCRETE

Kai YANG*, Changhui YANG, Adrian LONG, Muhammed BASHEER

Kai YANG is a research fellow at the School of Civil Engineering, University of Leeds, UK. Before this, he was a lecturer at the College of Materials Science and Engineering, Chongqing University, China. He received his BS and MS in 2005 and 2008 respectively from Chongqing University and PhD from Queen's University Belfast in 2012. His research interests include design and development of new permeation test methods, site quality control and assessment of durability of concrete in structures.

Changhui YANG, PhD, CEng, is a professor and the head of the College of Materials Science and Engineering, Chongqing University and the president of Chongqing Ceramic Society. His research interests include durability of concrete, alkali-activated binding materials, concrete admixtures and waste management.

Adrian LONG, PhD, DSc, OBE, FEng, FIAE, FICE, FIStructE, FIEI, FACI and FICT, is a professor emeritus at School of Natural and Built Environment, Queen's University Belfast, UK. He was the Dean of Engineering, at Queen's University Belfast and President of the ICE. His research interests include bridge engineering, structural performance, inspection and testing techniques.

Muhammed BASHEER, PhD, DSc, FEng, FIAE, FICE, FIStructE, FACI and FICT, is chair professor of structural engineering and the Head of School of Civil Engineering, University of Leeds, UK. He is a member of several international technical committees of the ACI and RILEM and a Council member of both the UK Concrete Society and Institute of Concrete Technology. His research interests include performance based specification, NDT test techniques, transport properties and sustainable materials technology.

USE OF A TWO PRESSURE-HEAD METHOD TO ASSESS THE WATER PERMEABILITY OF STRUCTURAL CONCRETE

ABSTRACT

Determining the water permeability of concrete in structures remains a conundrum because of difficulties in removing the influences of moisture. This study describes the extended flow-net theory developed on the basis of the two pressure head concept, which provides a means of measuring permeability under the partially saturated condition. Surface mounted tests and the standard laboratory water penetration tests were carried out to verify this approach. Before determining the water permeability, steady state flow rates at two different pressure levels were evaluated and the effects of initial moisture conditions on flow behaviour were investigated. The results indicate that the proposed approach does offer a useful means of determining the water permeability of structural concrete, although it cannot be claimed to be universally applicable for all moisture conditions likely to be encountered in practice.

Keywords: in situ water permeability, two pressure head test, extended flow-net theory, unsaturated flow

INTRODUCTION

Permeability of structural concrete is an essential parameter in the assessment of the durability of concrete structures (1-3). It can be measured through cores extracted from structures using laboratory methods (4, 5), but the cost is too high to get a statistically sound conclusion and the routine removal of cores could cause damage to the structure in terms of aggravating deterioration and/or depleting the structural capacity (3, 6). For this reason, many field permeability tests have been developed over time (1, 7-9). However, these methods often yield substantially dissimilar permeability values and one main reason is that permeability results are extremely sensitive to variations in moisture content of the concrete.

To control the effect of moisture, two main approaches have been utilised during the last decade. The first is to measure the moisture content and then adjust the permeability accordingly. Basheer and Nolan (10), and Parrott (11) recommended that to obtain reliable air permeability results the internal relative humidity of the near surface concrete should be less than 80%. The second approach is to remove moisture from the sample by certain pre-conditioning methods. Dhir et al. (12) suggested that vacuum dewatering could be used to eliminate the influence of moisture on results. Schonlin and Hilsdorf (13) used a hot air gun to dry out the moisture around test area prior to measurements. A high pressure was applied by Dinku and Reinhardt (14) to overcome the influence of moisture on air permeability tests. Most of the current research is focused on air permeability measurements, while relatively few studies were carried out to assess effects of moisture on water permeability tests. It is recognised that under the unsaturated condition, the rate of water flow at the concrete surface is influenced by both the permeability and the capillary effect (15, 16). The magnitude of the latter depends on a number of factors, e.g. the moisture content at the time of testing, the pore structure of concrete (17, 18). Therefore, the influence of unsaturated flow on results needs to be isolated to yield reliable estimation. To solve this problem, Hall and Hoff (15) suggested that in situ water permeability measurements can be carried out using two

pressure heads to separate the effect of moisture from results, but this concept needs to be investigated in relation to representative concrete specimens.

Based on the two pressure head concept, this study has developed the flow-net theory that analytically accounts for the influence of saturated and unsaturated flow. Results from experiments are presented to illustrate whether repeatable permeability results can be obtained using the proposed method under different test conditions. To assess the reliability of the proposed technique, two laboratory permeability test methods, the laboratory water penetration test and the air permeability test, were also carried out and the results from the new permeability test method and the laboratory test method were compared.

RESEARCH SIGNIFICANCE

With greater emphasis on the need for characterisation of durability of existing concrete structures, there is an increasing interest in the measurement of the permeation properties of near surface concrete. An important factor limiting the use of current test techniques is that the effect of moisture cannot be easily controlled or eliminated. Based on the concept proposed by Hall and Hoff (15), this study presents one approach to determine water permeability of concrete under partially saturated conditions. This method does not require assumptions concerning initial moisture content and offers one possible solution for removing the moisture influence.

PRINCIPLES AND GOVERNING RELATIONSHIP

The exact mathematical treatment of unsaturated flow is complex but it can, by approximation, be greatly simplified. The underlying principle of the proposed approach is the flow-net theory. One advantage is that the determination of the water permeability is not dependent on achieving a uni-directional flow (19, 20). In this theory, steady state flow into partial saturated concrete within a ring maintaining a constant pressure head is described using a pressure flux and a capillary flux based on Darcy's law:

$$q_s = \frac{Q_s}{\pi^2} = -K(\psi) \text{grad}(\psi) \Lambda \text{ m/s} \quad (1)$$

where q_s is the steady (or quasi-steady) volumetric flux (m/s); Q_s is the corresponding steady volumetric flow rate, the volume passing per unit time, (m^3/s); r is the ring radius (m); ψ is the total head (m), consisting of the hydraulic pressure of ponded water in the ring (H) and the capillary pressure of unsaturated concrete (ψ_i); $K(\psi)$ is the permeability-pressure relationship, which can be represented by the following model (15):

$$K(\psi) = K_s, \psi \geq 0 \quad (2-a)$$

$$K(\psi) = K_s g(\psi), \psi < 0 \quad (2-b)$$

where K_s is the saturated permeability (m/s).

Then, Eq (1) can be simplified using a generalised flux potential:

$$\Phi = \int_{\psi_i}^H K(\psi) d\psi \Lambda \text{ m}^2/\text{s} \quad (3)$$

where Φ is the generalised flux potential (m^2/s) and Eq (1) becomes:

$$q_s = -K(\psi) \text{grad}(\psi) = -\text{grad}(\Phi) \Lambda \text{ m/s} \quad (4)$$

Using mass balance, the total flow (Q_s) out of the ring can be written as:

$$Q_s = \int_{A_s} -q_s dA_s = \int_{A_s} \text{grad}(\Phi) dA_s \Lambda \text{ m}^3/\text{s} \quad (5)$$

where A_s is the area of the ponded surface (m^2).

By assuming that unsaturated concrete is a rigid, homogeneous, isotropic and semi-infinite porous media, total flow (Q_s) can be estimated using the flow-net theory (19, 20):

$$Q_s = C\Phi_s, C = \frac{2\pi n_f}{n_d} \times \frac{ab}{l} \quad (6)$$

where C is a shape factor (m) that can be determined based upon the water flow patterns (see **Fig. 1**), for which detailed calculation procedures have been reported in previous studies (19, 20); Φ_s is the total flux potential (including both pressure and capillary potential); n_f is the number of paths (flow channels); n_d is the number of equipotential drops; a is the distance normal to symmetry axis (m); b is the width of flow path (m); l is the distance between equi-potentials (m).

As indicated in Eq (2) and (3), the total flux potential (Φ_s) can be expressed to

$$\Phi_s = \int_{\psi_i}^H K(\psi) d\psi = \int_0^H K(\psi) d\psi + \int_{\psi_i}^0 K(\psi) d\psi = K_s H + \Phi_c \quad (7)$$

where Φ_c is the flux potential representing the effect of capillarity of unsaturated concrete,

$$\text{equivalent to } \int_{\psi_i}^0 K(\psi) d\psi = \int_{\psi_i}^0 K_s g(\psi) d\psi = \Phi_c.$$

Substituting Eq (7) into (6) produces:

$$Q_s = C \Phi_s = C (K_s H + \Phi_c) \Lambda \quad (8)$$

This relationship indicates that two main components affect steady-state flow: flow due to the hydrostatic pressure ($K_s H$) and flow due to capillary suction of the unsaturated concrete (Φ_c). Note that this equation cannot be solved without additional information of K_s and Φ_c .

According to Hall and Hoff (15), two pressures can be successively applied in the measuring ring to generate two simultaneous equations. Supposing two pressures (H_1 and H_2) are used and the resulting steady-state flow rates (Q_1 and Q_2) are measured, the solution of Eq (8) is:

$$K_s = \frac{Q_2 - Q_1}{C(H_2 - H_1)} \Lambda \quad (9-a)$$

$$\Phi_c = \frac{Q_1 H_2 - Q_2 H_1}{C(H_2 - H_1)} \Lambda \text{ m}^2/\text{s} \quad (9-b)$$

where Q_1 and Q_2 are the steady-state flow rates (m^3/s) corresponding to H_1 and H_2 respectively ($H_2 > H_1$). Physically, K_s represents the property of concrete, water permeability, and the effect of capillary on flow equals Φ_c . The proposed extended flow-net theory provides a tool for gaining insights into the problem of unsaturated flow and through the use of two different pressure a means of solving Eq (9).

EXPERIMENTAL PROGRAMME

Raw materials and concrete

The concrete studied was made with a water to cement (W/C) ratio of 0.375. Mix proportions are reported in **Table 1**. Portland cement used in this project was manufactured by Lafarge and conformed to GB-175 (21). The superplasticiser was a polycarboxylic acid based polymer in accordance with GB-8076 (22).

The fine aggregate was medium graded natural sand and the coarse aggregate crushed basalt with 10 mm [0.39 in.] and 20 mm [0.78 in.] size proportioned in equal mass. The moisture condition of the aggregates was controlled by pre-drying in an oven at $105(\pm 5)^\circ\text{C}$ [$221\pm 9.0^\circ\text{F}$] for 24 hours followed by cooling to $20(\pm 2)^\circ\text{C}$ [$68\pm 3.6^\circ\text{F}$] for one day before concrete preparation.

The basic properties of concrete (slump, air content and compressive strength) were tested and are also reported in **Table 1**.

Preparation of the specimens

Six $300 \times 250 \times 150 \text{ mm}^3$ [$11.81 \times 9.84 \times 5.91 \text{ in.}^3$] slabs were manufactured, which were divided into three groups for different curing regimes. According to the simulation of water flow in the previous study, the water flow is a combined function of specimen thickness and testing area. The diameter

of the testing area in this study is 50 mm and beyond 40 mm depth from the testing surface water flow would be very small. As such, 150 mm thickness was selected to eliminate the influence of geometry of specimen on results. The mixing procedure was based on BS-1881: part 125 (23). Concrete was compacted using a poker and compaction was considered to have been completed when no air bubbles rose to the surface of concrete. After compaction, the specimens were covered with plastic sheets immediately and were removed from the mould after 24 hours. To remove any influence of cement hydration on permeability test results, they were cured as follows until the age of 90 days:

- Air cured (designation AC): air-stored in a controlled environment (20 ± 2 °C [68 ± 3.6 °F], $50 \pm 10\%$ RH) after demoulding.
- Sealed cured (designation SC): wrapped by plastic sheets and moved to a temperature controlled environment (20 ± 2 °C [68 ± 3.6 °F]) after 3-day water curing.
- Moisture cured (designation MC): transferred into a fog room (20 ± 2 °C [68 ± 3.6 °F]) after demoulding until test.

Three curing regimes were selected to produce different permeability properties especially for the near surface region (3, 13, 24). The proposed water permeability tests were carried out on the 300×250 mm² [11.81×9.84 in.²] surface.

Initial moisture conditions of the water permeability tests

The aim of this research was to validate if the proposed approach can yield repeatable and reliable water permeability results under different initial conditions. It is therefore of interest to vary initial moisture conditions experimentally and to study the performance of the proposed approach. To achieve this, four initial conditions were investigated:

- Condition 1 (designation C1): at the age of 90 days after being cured.

- Condition 2 (designation C2): after C1, samples were placed on the supports in a container, in which water was filled to 5 mm above the test surface, and after water absorption for 2 days the permeability tests were carried out.
- Condition 3 (designation C3): after C2, samples were dried in an environment controlled environment (20 ± 2 °C [68 ± 3.6 °F], $50 \pm 10\%$ RH) for 3 days.
- Condition 4 (designation C4): after C3, samples were dried in an environment controlled environment (20 ± 2 °C [68 ± 3.6 °F], $50 \pm 10\%$ RH) for another 7 days.

Figure 2 summarises the curing regimes and the initial moisture conditions. Water permeability of concrete was tested under the 12 combinations of test conditions and three replicates were carried out for each condition.

Experimental devices and measurements

Surface mounted water permeability test

The water permeability test used in this study was based on the surface mounted permeability tests (1, 20). **Figure 3** shows the test instrument, details of which are available in the previous study (20). The test set-up was calibrated before carrying out measurements on the concrete. At the beginning, a cylinder at the top of the head which supplies water to the test region was filled with water. The test head was then clamped onto a given specimen and water was admitted by a syringe through the tube, as shown in **Fig. 3-b**. The test system was then pressurised using compressed air. Once the pressure in the test system was slightly above 1 bar [14.5 psi], the initial pressurisation was complete and a volume reading was recorded as the initial value ($t=0$ min). As water ingressed into the concrete during tests, pressure inside the test head decreased. To maintain the pressure at 1 bar [14.5 psi], the piston was manually advanced, which was used to record the volume of water penetrating into the concrete every minute. After 80 mins, the test pressure was increased to 2 bar

[29 psi], while the measuring process was repeated for another 80 mins. At the end of 160 mins of test period, the measurement was considered to have been completed.

The extended flow net theory requires that the region of concrete being tested has a similar moisture profile and isotropic water permeability. Therefore, to remove influences of possible heterogeneity encountered between pressures 1 and 2, the test duration to reach quasi-steady state flow was selected based on previous experience (19, 20).

Surface-mounted air permeability test

Figure 4 shows the surface mounted air permeability test instrument used in this study to examine the air permeability of the near-surface concrete, further details of which have been reported in the literature (10,17,18). The test area considered was the inner 50 mm circle, isolated using a base ring, of the 100 mm cylindrical specimens cut from the 300×250×150 mm³ [11.81×9.84 ×5.91in.³] slabs. To remove the influence of moisture on air permeability, the specimens were placed in the drying cabinet at 40 °C until constant mass (M_{40C}) was achieved. The instrument was pressurised manually by a syringe and when the pressure in the test chamber reached 0.5 bar (7.25psi), the test commenced automatically. The pressure inside the test chamber then decreased due to air escaping through the pores in the specimen. The rate of pressure decay was monitored every minute for 20 minutes, which was used to compute the air permeability index, API (unit: ln(bar)/min) using the following equation:

$$API = \frac{\ln \frac{P_i}{P_t}}{t_t - t_i} \quad (10)$$

where t is the time (s); P_i and P_t (N/m²) are the pressures in the chamber at the start and at any time, t , respectively. Three samples were tested for each concrete.

BS-EN water penetration test

Water penetration test according to BS-EN: 12390-8 (25) was carried out to verify conclusions derived from the proposed method. Three 100 mm [3.94 in.] diameter cores extracted from the from the 300×250×150 mm³ [11.81×9.84 ×5.91in.³] slab specimens were tested for each concrete mix. The test set up is illustrated in **Fig. 5**. A constant test pressure of 7.0 bar [101.5 psi] was applied for three days using compressed air at one end of the test specimen. At the end of the test, specimens were split open and the depth of water penetration measured. The average value of penetration depth is reported.

RESULTS AND DISCUSSION

Determination of steady-state flow rate under two pressure heads

The computation of water permeability using the extended flow-net theory needs steady state flow rates under the two different pressure levels to be determined before conducting the following analysis. In this study, steady-state flow rates are assumed to be attained when two requirements are satisfied (19, 20): one is that a linear relationship exists between the volume of water penetrating into the concrete and the elapsed time; and the other is that there is no significant variation in the flow rates during a specific period of time. To verify these two aspects, the following approach was used:

- Plot the water volume against the elapsed time to obtain overall flow behaviours under two pressure levels.
- Determine the flow rates through regression analysis at interval of 10 min and graphically display to illustrate the relative change.
- Compare the variation of flow rates and identify the period for water flow to reach the steady state flow.

Due to similarity of the general responses, three sets of results were selected and presented as an example of interpretation in this section. The specimens were air cured (AC), sealed cured (SC) and

moisture cured (MC). The test condition was after 90-day curing (C1). **Figure 6** gives the volume of water and the flow rates against elapsed time. Note that the scale in **Fig. 6** for zoomed in part of the data is different for the different test conditions, but it depended on the main influencing factors, the curing regime and the initial condition. The same scale for the curing regime, 300 μL for MC, 600 μL for SC and 2200 μL for AC, is used to examine the influence of initial moisture conditions. Meanwhile, the differences between three curing regimes can be easily identified in three different scales. The analysis of **Fig. 6** is based on the pressure applied:

First stage (pressure-1 from 0 to 80 min): initially, the relationship between the volume of water flowing into concrete and time is not linear for all three cases. This phenomenon is not surprising to be observed, as unsaturated water flow rate and time are not linearly related at the start (15, 26, 27). However, curvatures of the water volume versus time plots were comparatively small after 60 min and variations of the flow rates became small. Furthermore, the regression coefficients were close to a value of one. This observation agrees with results reported previously (20).

Second stage (pressure-2 from 80 to 160 min): after 80 mins, the test pressure was increased to 2 bar [29 psi]. As shown in **Fig. 6**, the general trend for the second pressure is similar to the first pressure. The volume of water entering into the concrete also displays a nonlinear relationship with time and flow rates gradually declines, but no significant reduction occurred after 40 mins (in total 120 min).

Another feature noticed in **Fig. 6** is that the flow at 2 bar [29 psi] shows uncertainties at the initial stage (from 80 to 120 min). For MC, flow rates were around $1.4 \times 10^{-9} \text{m}^3/\text{min}$ [$8.54 \times 10^{-5} \text{in.}^3/\text{min}$], slightly above the flow rate ($1.1 \times 10^{-9} \text{m}^3/\text{min}$ [$6.71 \times 10^{-5} \text{in.}^3/\text{min}$]) at 1 bar [14.5 psi], while an increase in pressure did not give a higher flow rates for SC and AC at the beginning. As indicated in Eq (8), flow rates are a function of capillary suction (Φ_C) and hydraulic pressure (H). Although the test location was not changed and variance due to the test location was controlled, the moisture content at the second pressure was different from the first pressure. After 1 bar [14.5 psi] testing,

the moisture content in the surface region increased, meaning a reduction in capillary suction at the 2 bar [29 psi] test. Meanwhile, the effect of hydraulic pressure is less significant and the capillary suction governed flow features at the start, as illustrate in **Fig 6. (a)** (15, 17). As such, it is possible to observe lower flow rates at 2 bar [29 psi] due to decreases in capillary suction. For the three cases, the flow rates at 2 bar [29 psi] were higher than those for 1 bar [14.5 psi] after 120 min. This is because the impact of capillary suction decreases as time increases and the hydraulic pressure begins to dominate the overall flow response. Furthermore, regression coefficients were greater than 0.98. Therefore, the corresponding quasi-steady state flows for pressures 1 and 2 can be determined using data recorded between 60-80 and 140-160 mins respectively.

Effects of initial moisture condition on behaviour of unsaturated flow

Figure 7 gives results of the water permeability tests under the 12 test conditions, which result from three curing regimes under four initial conditions. For ease of comparison under different combinations, different scales of y-axis were used. As shown in **Fig. 7**, the difference of volume of water flowing into the concrete is above one order of magnitude and for all 12 combinations a constant flow rate is almost impossible for the first 60 min, while beyond this point the volume is roughly proportional to time for both pressure conditions. Consequently, the steady flow rates were evaluated based on regression analysis described in the previous section.

Steady state flow rates under four different initial conditions have been plotted against the pressure in **Fig. 8**. Average steady state flow rates obtained for all concretes were relatively low, ranging from 0.10 to $8.9 \times 10^{-9} \text{m}^3/\text{min}$ [6.10×10^{-6} to $5.43 \times 10^{-4} \text{in.}^3/\text{min}$]. It is clear that in all cases (C1-C4), the flow rates of AC are much higher than those of MC and SC. This links in the fact that the three curing regimes resulted in different permeation properties and initial moisture contents at near surface concrete (28, 29). MC refers to the moisture cured concrete, under which condition additional moisture was present in the concrete and no significant drying occurred from the surface in the whole curing period. The moisture content in the surface region was sufficient to yield low

permeability (12, 14). With respect to SC, concrete was sealed after 3 day water curing. That is, curing was also in a good condition, but the moisture content was relatively less than MC due to hydration (4, 24). For AC, concrete was moved to a controlled environment condition (20°C [68 F], 50%RH) after demoulding and no additional water was provided. It can be deduced that AC has the lowest moisture content and the highest permeability. Against these backgrounds, it is reasonable to observe that flow rates of AC are significantly greater than the other two concretes.

Clearly from **Fig 8-a**, concretes after curing (C1) gives the highest flow rates, especially for SC and AC. This is due to the strong capillary suction caused by comparatively low moisture content. As indicated in Eq (8), the unsaturated component (Φ_C) can exert an important influence on flow rate under the dry condition. After 2 day water absorption (C2), values of capillary suction significantly decreased (16, 27). As such, a significant reduction in flow rate was found in **Fig. 8**. Comparison of flow rates of SC and AC between C1 and C2 also indicates that SC has a much higher relative decrease (more than 80%) after ponding (C2) despite of a less absolute decrease. This implies that flow of SC was mainly caused by capillary suction, while the pressure contributed relatively less to the total flow. It can be deduced that water permeability might be slightly overestimated in porous concrete (AC), but significantly overestimated in dense concrete (MC and SC), if the unsaturated component (Φ_C) is not considered.

Further, it is clear from **Fig. 8** that effects of drying after water absorption (C3 and C4) depended upon the nature of concrete studied. Flow rates of AC showed a steady increase as drying duration increased, while no clear trend can be found for MC and SC. Based on Eq (7), for the two parts of steady state flow (K_{sH} and Φ_C), the value of the K_{sH} is unaffected by variations of the moisture content, but the extent of flow rate which the Φ_C will influence relies on the value of capillary pressure (ψ_i) and unsaturated permeability ($K(\psi)$). AC has a porous and permeable surface (higher $K(\psi)$), meaning the moisture loss was faster than the other two. This naturally resulted in higher capillary pressure (ψ_i), yielding an increase in the flow rates for drying from 3 days to 10

days (4, 24). However, a denser surface of MC and SC makes the drying process slow, which could cause a limited increase in capillary pressure (ψ_i). Along with the lower permeability, the flow rates of these two concretes seem not to be sensitive to drying.

Example calculation of water permeability and capillarity using the two pressure head approach

The primary aim of this study was to justify if the two pressure head approach can be used to estimate in situ water permeability (K_s) and capillary effect (Φ_C). To show procedures of determining these two parameters, an example of calculation is provided next:

- Environmental conditions in the laboratory during the measurement: Temperature 18.7 °C [65.66 °F]; Relative humidity 53%.
- Curing regime: air cured (AC).
- Initial moisture condition: after air curing for 90 days (C1).
- Age of concrete: 90 days.
- Test parameters:

Radius of the test area: 0.025 m [0.984 in.].

Calibration factor: $C=122.31$ m [4815.35 in.] determined from the pattern of flow net (19, 20).

Pressure applied: $H_1=1$ bar [14.5 psi] (10.336 m [406.93]) and $H_2=2$ bar [29 psi] (20.672 m [813.86 in.])

- Steady state flow rates:

1 bar [14.5 psi]: $Q_1=6.42 \times 10^{-9}$ m³/min= 1.070×10^{-10} m³/s [6.53×10^{-6} in.³/s]

2bar [29 psi]: $Q_2=8.94 \times 10^{-9} \text{ m}^3/\text{min}= 1.491 \times 10^{-10} \text{ m}^3/\text{s} [9.10 \times 10^{-6} \text{ in.}^3/\text{s}]$

- Calculation:

$$K_s = \frac{Q_2 - Q_1}{C(H_2 - H_1)} = \frac{1.491 \times 10^{-10} - 1.070 \times 10^{-10}}{122.31 \times (20.672 - 10.336)} = 3.32 \times 10^{-14} \text{ m/s} [1.31 \times 10^{-12} \text{ in./s}]$$

$$\Phi_c = \frac{Q_1 H_2 - Q_2 H_1}{C(H_2 - H_1)} = \frac{20.672 \times 1.070 \times 10^{-10} - 10.336 \times 1.491 \times 10^{-10}}{122.31 \times (20.672 - 10.336)} = 5.32 \times 10^{-13} \text{ m}^2/\text{s} [8.25 \times 10^{-10} \text{ in.}^2/\text{s}]$$

Assessment of reliability of two pressure head technique

Average values of water permeability (K_s) and capillarity (Φ_c) determined by the proposed method are shown in **Fig. 9**. For the three curing regimes, the values of water permeability (K_s) under four initial moisture conditions are reasonably consistent and do not show any marked trend, which means the proposed approach is able to give repeatable results under different initial moisture conditions. The results, therefore, can be used in the following discussion.

As expected, no significant difference in water permeability of SC and MC can be found, while AC has much larger water permeability than the other two. It confirms the effect of curing on permeability (4, 24). To verify this observation, the results of the water penetration test and the air permeability test were compared, which are reported in **Table 2**. Note that the penetration depth was not used to calculate the water permeability coefficient, but as a parameter to qualitatively reflect water permeability of the tested concretes. This is because for a non-steady state water permeability test, permeability coefficient is a combination of permeability coefficient and accessible porosity in the test region (17, 30), meaning that the permeability coefficients determined from the steady-state method and the non-steady state method may not be compared directly. As seen in **Table 2**, the water penetration front for AC is about 6 times higher than MC or SC, while the penetration depths of MC and SC are of comparable magnitude. Similar trend was also observed

for air permeability. Considering the inherent variance of the concrete permeability, it can be concluded that a similar conclusion can be obtained for three permeation test methods.

Examination of capillarity (Φ_C) shows that this parameter is highly variable under different initial conditions. Very limited information about this parameter is available for the present study, but from a physical point of view, this trend is perhaps not surprising, as pressurised flow tends to maximise the hydrostatic pressure components of flow (K_s) rather than the capillary component (Φ_C). Another important feature noted in **Fig. 9** is that four unrealistic negative values of capillarity (Φ_C) are found among the twelve test conditions. This discrepancy made it desirable to investigate reasons behind, as the proposed approach is not able to yield realistic results in some cases.

According to Eq (9), for the valid results, i.e. positive water permeability (K_s) and the capillarity (Φ_C), the value of Q_2 should be in the region between Q_1 and $2Q_1$. In mathematical terms, if Q_2 is less than Q_1 , the water permeability (K_s) becomes negative, while the negative capillarity (Φ_C) would be found, if Q_2 is higher than $2Q_1$. **Figure 8** clearly shows that Q_2 is always higher than Q_1 , meaning positive water permeability (K_s). However, values of Q_1 are very low for four conditions, viz. MC-C1, MC-C2, SC-C2, AC-C2, under which conditions negative values of capillarity (Φ_C) are found. These observations may be due to the moisture distribution. As indicated previously, water absorption is able to remove the effect of capillary suction, but only the top surface layer is saturated by this treatment (13, 28). If the water flow remained in the top surface region during the 1 bar [14.5 psi] test, where capillary effect was insignificant, a low flow rate was generally observed. As time elapsed and a higher testing pressure was applied, water moved deeper and beyond the top region, where unsaturated flow may dominate the overall response, leading to a greater flow rate. This suggests that the proposed equations cannot be applied if the moisture content at the test surface is wet.

The results indicate that for a wet surface, 10 day drying is helpful to obtain an acceptable condition for a reliable measurement, as both water permeability (K_s) and capillarity (Φ_C) become positive

for C4. It suggests that the two pressure head approach can be reliable in assessing water permeability of near surface concrete under partially saturated condition, provided the test surface is relatively dry.

CONCLUSIONS

Assessment of in situ water permeability is a difficult task due to the range of influencing factors involved. Of primary difficulty is an approach to eliminate the effect of moisture. Hall and Hoff suggested a two pressure head technique to address this challenge. On the basis of this idea, the flow-net theory was developed to analyse partially saturated flow and verification of the proposed method was carried out. The following conclusions have been drawn:

1. Measurement of the steady state flow rates at the two pressure heads permits the calculation of the water permeability through a direct application of the extended flow-net theory and the results indicate that relatively consistent water permeability can be obtained under different initial conditions.
2. Reliability of the proposed approach was assessed by comparing with the water penetration test and surface-mounted air permeability test. It was found that the new method can yield a trend similar to the other two permeability test methods.
3. Water flow is very sensitive to the moisture content at the test surface and can lead to meaningless results (negative Φ_C) on a wet surface. From a practical point of view and current results, it is recommended that both water permeability (K_s) and capillarity (Φ_C) are determined and results can be considered to be valid and accurate when both parameters are positive.
4. With respect to a wet test surface, pre-drying is useful in order to achieve reliable data and the preliminary results indicate that drying for 10 days (20 °C [68 °F], 55% relative humidity) may be sufficient to precondition the test surface.

Although some encouraging results have been obtained, more research work needs to be carried out to further verify this approach. Future work will focus on establishment of the relationship between the test pressure and the steady-state flow rate to refine the test method, and estimation of the variability of structural concrete.

ACKNOWLEDGEMENTS

The experiments described in this paper were carried out in the concrete laboratory of Chongqing University and the authors acknowledge Chongqing University for providing facilities for the investigation reported in this paper. The authors thank financial supports provided by National Natural Science Foundation of China (Project No. 51408078), and the open Funds from both State Key Laboratory of High Performance Civil Engineering Materials and Shenzhen University. The supports from Queen's University Belfast and University of Leeds are also greatly appreciated.

REFERENCES

1. Torrent RT, "A two-chamber vacuum cell for measuring the coefficient of permeability to air of the concrete cover on site," *Materials and Structures*, V. 25. 1992, pp. 358-365.
2. Andrade C, Gonzalez-Gasca C, Torrent R, "Suitability of Torrent Permeability Tester to Measure Air-Permeability of Covercrete," *ACI Special Publication-192*, 2000, pp. 301-317.
3. Long AE, Henderson GD, Montgomery FR, "Why assess the properties of near-surface concrete," *Construction and Building Materials*, V. 15. 2001, pp. 65-79.
4. Bungey JH, Millard SG, Grantham MG, "Testing Concrete in Structures." 4th ed. Taylor and Francis; 2006.
5. Goodspeed CH, Vanikar S, Cook A, "High-Performance Concrete Defined for Highway Structures," *Concrete International*, V. 18. 1996, pp. 62-67.

6. Tang L, Nilsson LO, Basheer PAM, "Resistance of Concrete to Chloride Ingress: Testing and modelling." Spon Press; 2011.
7. Wong HS, Pappas AM, Zimmerman RW, Buenfeld NR, "Effect of entrained air voids on the microstructure and mass transport properties of concrete," *Cement and Concrete Research*, V. 41, No. 10. 2011, pp. 1067-1077.
8. Parrott LJ, "Water absorption in cover concrete," *Materials and Structures*, V. 25. 1992, pp. 284-292.
9. Figg JW, "Methods of measuring the air and water permeability of concrete," *Magazine of Concrete Research*, V. 25. 1973, pp. 213-219.
10. Basheer PAM, Nolan EA, "Near-surface moisture gradients and in situ permeation tests," *Construction and Building Materials*, V. 15. 2001, pp. 105-114.
11. Parrott LJ, "Moisture conditioning and transport properties of concrete test specimens," *Materials and Structures*, V. 27. 1994, pp. 460-468.
12. Dhir RK, Hewlett PC, Brars EA, Shaaban IG, "A new technique for measuring the air permeability of near-surface concrete," *Magazine of Concrete Research*, V. 47. 1995, pp. 167-176.
13. Schonlin K, Hilsdorf HK, "Evaluation of the effectiveness of curing of concrete structures," *ACI Special Publication-100*, 1987, pp. 207-226.
14. Dinku A, Reinhardt H, "Gas permeability coefficient of cover concrete as a performance control," *Materials and Structures*, V. 30. 1997, pp. 387-393.
15. Hall C, Hoff WD, "Water transport in brick, stone and concrete." Spon Press; 2012.

16. Martys NS, Ferraris CF, "Capillary transport in mortars and concrete," *Cement and Concrete Research*, V. 27. 1997, pp. 747-760.
17. Technical Report No.31, "Permeability testing of site concrete: A review of methods and experience," Concrete Society, City, 2008, pp. 1-80.
18. Basheer PAM, "Permeation analysis," *Handbook of Analytical Techniques in Concrete Science and Technology: Principles, Techniques and Applications*, Noyes Publications, 2001, pp. 658-727.
19. Adams AE, "Development and application of the CLAM for measuring concrete permeability", PhD Thesis, Queen's University Belfast, Belfast, 1986.
20. Yang K, Basheer PAM, Bai Y, Magee BJ, Long AE, "Assessment of the effectiveness of the guard ring in obtaining a uni-directional flow in an in situ water permeability test," *Materials and Structures*, 2013. DOI: 10.1617/s11527-013-0175-5
21. GB-175, "Common Portland cement," Standardization Administration of the People's Republic of China, SAC, 2007, 16 pages.
22. GB-8076, "Cement admixtures," Standardization Administration of the People's Republic of China, SAC, 2008, 17 pages.
23. BS:1881-125, "Methods for mixing and sampling fresh concrete in the laboratory," BSI, 1986, 10 pages.
24. Aitcin PC, "High performance concrete." Spon Press; 1998.
25. BS-EN:12390-8, "Testing hardened concrete Depth of penetration of water under pressure," BSI, 2009, 10 pages.

26. Hall C, "Water sorptivity of mortars and concretes a review," Magazine of Concrete Research, V. 41. 1989, pp. 51-61.
27. McCarter W, Emerson M, Ezirim H, "Properties of concrete in the cover zone developments in monitoring techniques," Magazine of Concrete Research, V. 47. 1995, pp. 243-251.
28. Galle C, Daian JF, "Gas permeability of unsaturated cement-based materials application of a multi-scale network model," Magazine of Concrete Research, V. 52. 2000, pp. 251-263.
29. Potter R, Ho DWS, "Quality of Cover Concrete and its Influence on Durability," ACI Special publication-100, 1987, pp. 423-446.
30. Bamforth PB, "The relationship between permeability coefficients for concrete obtained using liquid and gas," Magazine of concrete research, V. 39, No. 138. 1987, pp. 3 -11.

TABLES AND FIGURES

List of Tables

Table 1 Mix proportions and general properties of concrete tested

Table 2 Results of water penetration depth and air permeability index

List of Figures

Fig. 1 Illustration of basic information and a flow-net determined from a model

Fig. 2 Illustration of curing regimes applied and different initial moisture conditions

Fig. 3 Surface mounted water test instrument

Fig. 4 Surface mounted air permeability test instrument

Fig. 5 Water penetration test instrument

Fig. 6 Graphical interpretation of flow behaviours

Fig. 7 As received data for three curing regimes under four different initial conditions

Fig. 8 Steady state flow rates for four different initial moisture conditions

Fig. 9 Results of the water permeability and capillarity under different initial moisture conditions

Table 1 Mix proportions and general properties of concrete tested

Concrete	Value
Cement (kg/m ³)	400
Water (kg/m ³)	150
Sand (kg/m ³)	700
Coarse aggregate (kg/m ³)	1090
Superplasticiser (percentage by mass of the cement content)	1.1
Slump (mm)	195
Air content (%)	1.2
28 day Compressive strength (MPa)	68.6
56 day Compressive strength (MPa)	74.9

(Note: 1 kg/m³= 0.0624 lb/ft³; 1MPa= 1.45×10⁻⁷ psi; 1mm= 0.039 in.)

Table 2 Results of water penetration depth and air permeability index

Curing regime applied	Air permeability index (Ln(bar)/min)	Water penetration depth (mm)
MC	0.083	5.1
SC	0.094	4.8
AC	0.135	31.4

(Note: MC, SC and AC are defined in Fig. 2; 1mm= 0.039 in.; 1 bar = 14.5 psi)

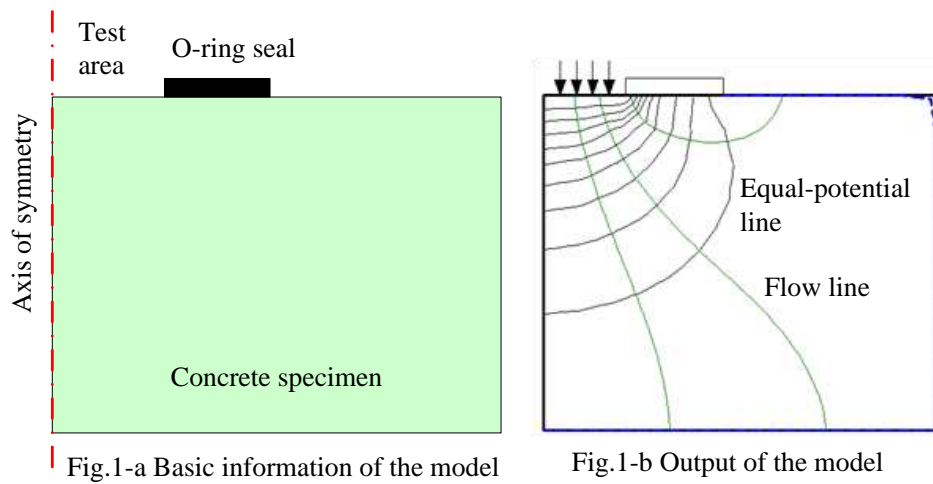


Fig. 1 Illustration of basic information and a flow-net determined from a model

		Initial moisture conditions			
		M1	M2	M3	M4
Moisture cured (MC)	Frog room to 90 days	2 d water absorption	Dry for 3d	Dry for 7d	
Sealed cured (SC)	3 d in water Sealed cured to 90 days	2 d water absorption	Dry for 3d	Dry for 7d	
Air cured (AC)	Air cured to 90 days	2 d water absorption	Dry for 3d	Dry for 7d	

Note:

1. Curing regime applied: MC refers to moisture cured; SC refers to sealed cured; AC refers to air cured.
2. Initial moisture condition: C1 refers to specimens after curing for 90 days; C2 refers to specimens after 2 day water absorption; C3 refers to specimens room dried for 3 days after water absorption; C4 refers to concrete room dried for 10 days after water absorption.

Fig. 2 Illustration of curing regimes applied and different initial moisture conditions

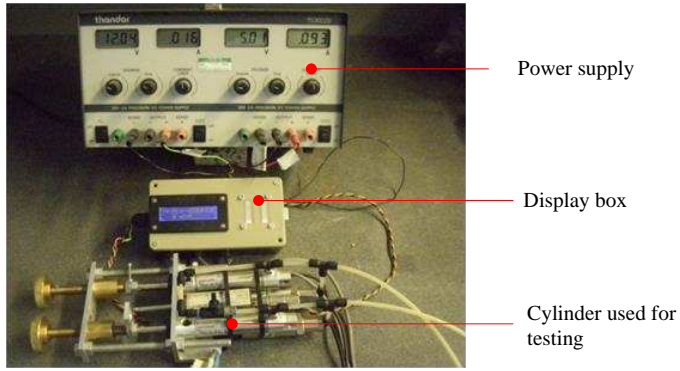


Fig.3-a The measuring unit of the instrument

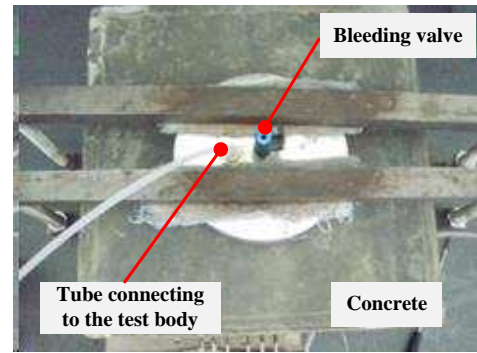


Fig. 3-b Illustration of the clamped test head

Fig. 3 Surface mounted water test instrument

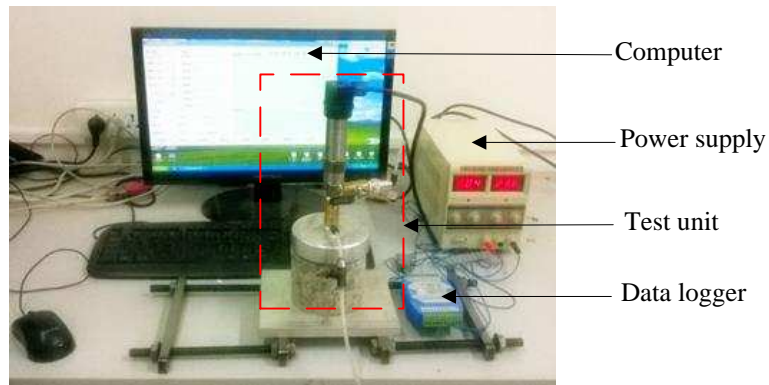


Fig. 4 Surface mounted air permeability test instrument

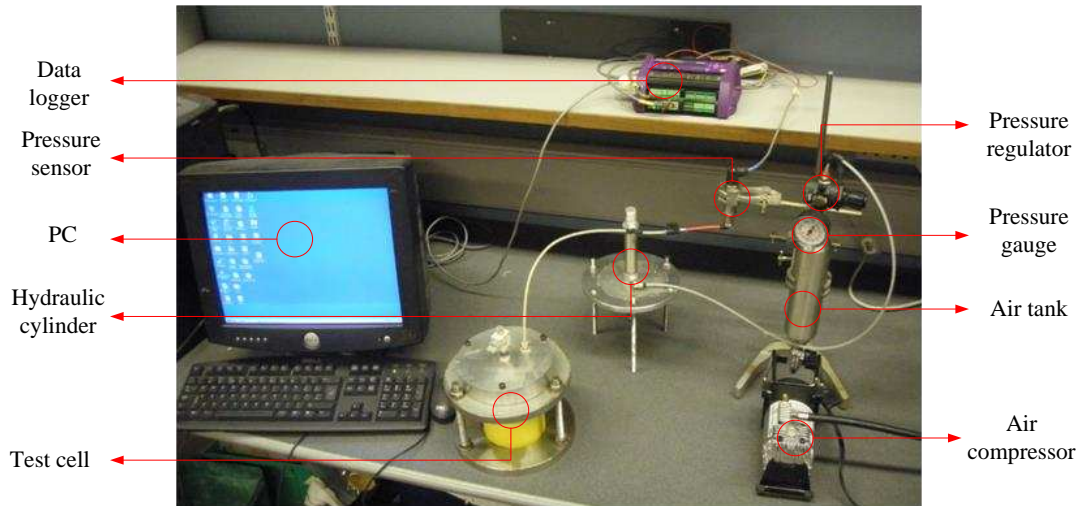


Fig. 5 Water penetration test instrument

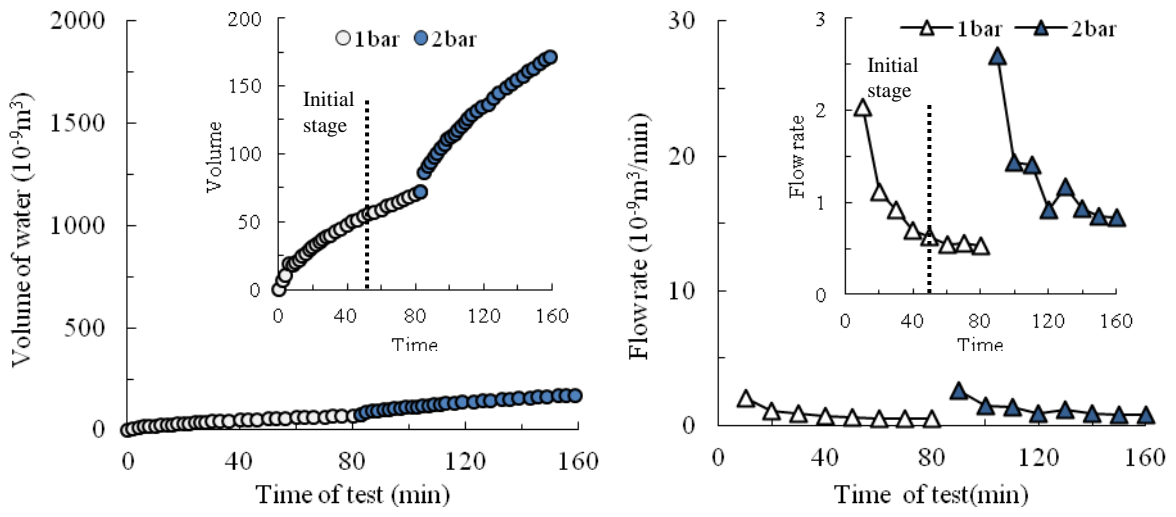


Fig. 6-a Moisture cured concrete (MC)

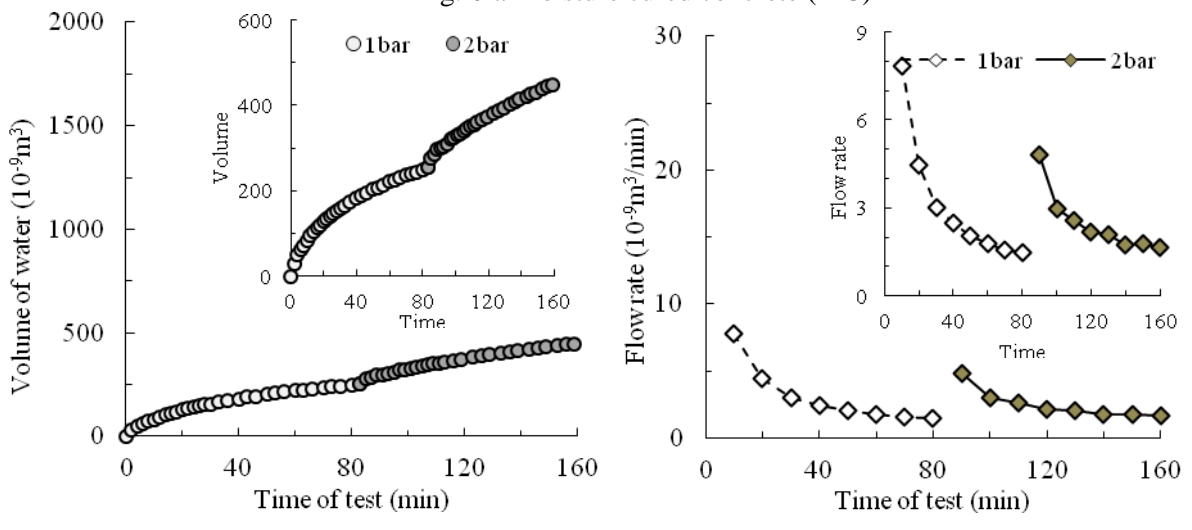


Fig. 6-b Sealed cured concrete (SC)

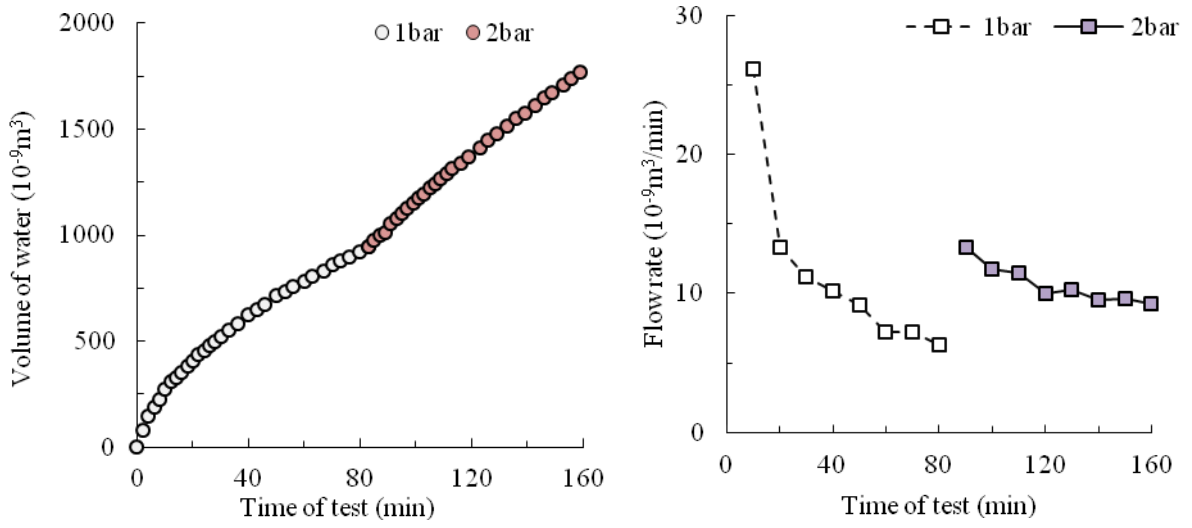
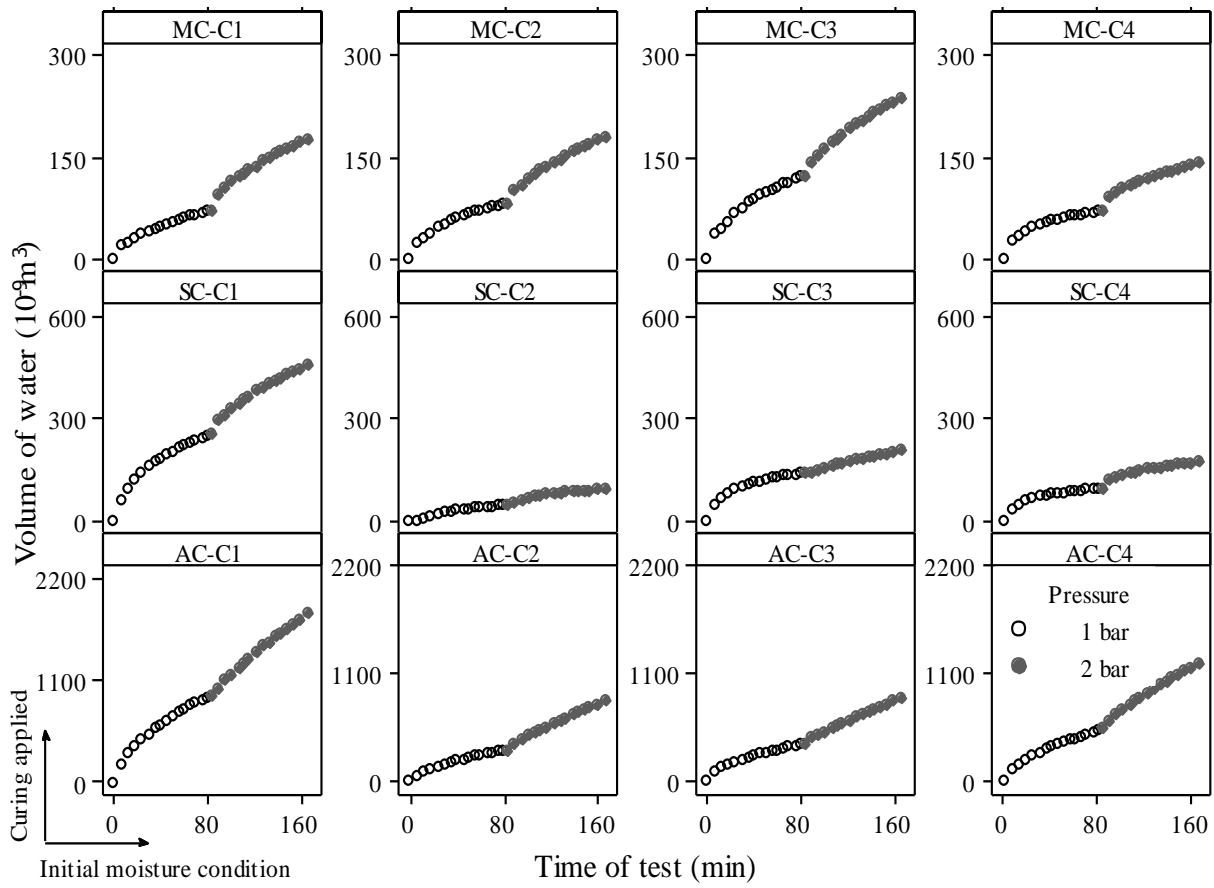


Fig. 6-c Air cured concrete (AC)

Fig. 6 Graphical interpretation of flow behaviours

(Note: $1 \text{ m}^3 = 6.10 \times 10^4 \text{ in.}^3$)



Note:

1. Initial moisture condition: C1 to C4 are defined in Fig. 2.
2. Curing regimes applied: MC, SC and AC are defined in Fig. 2.

**Fig. 7 As received data for three curing regimes under four different initial conditions
(Note: 1 m³=6.10×10⁴ in.³)**

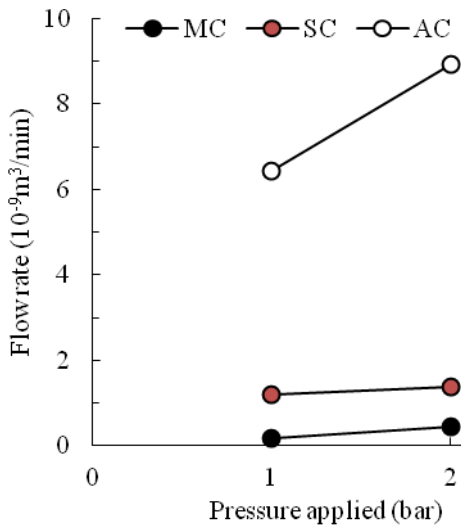


Fig.8-a: C1

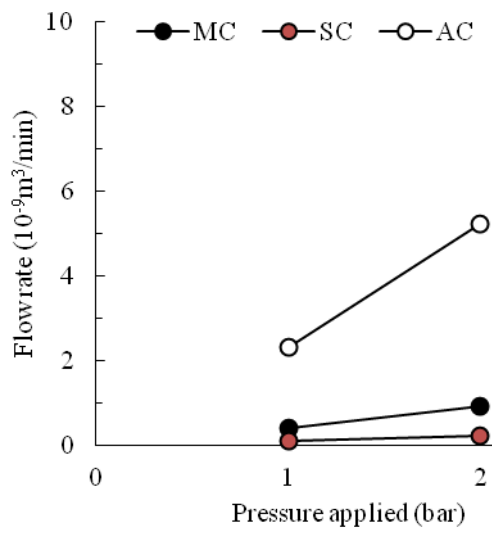


Fig.8-b

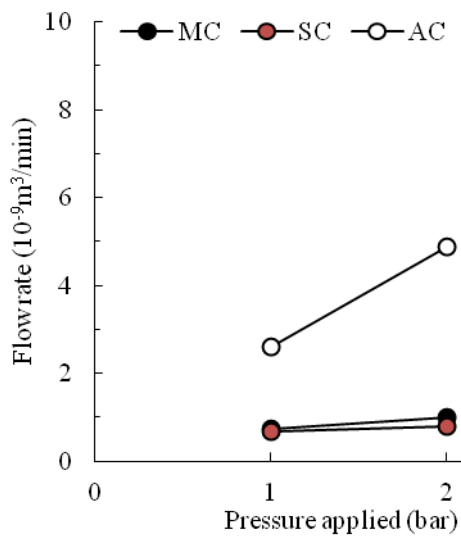


Fig.8-c: C3

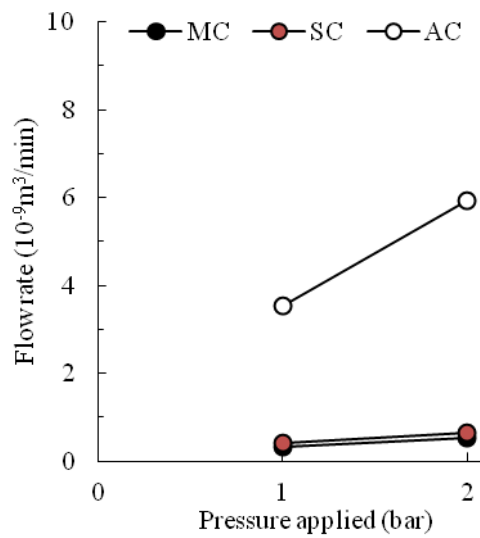


Fig.8-d: C4

Note:

1. Initial moisture condition: C1 to C4 are defined in Fig. 2.
2. Curing regimes applied: MC, SC and AC are defined in Fig. 2.

Fig. 8 Steady state flow rates for four different initial moisture conditions

(Note: 1 m³=6.10×10⁴ in.³)

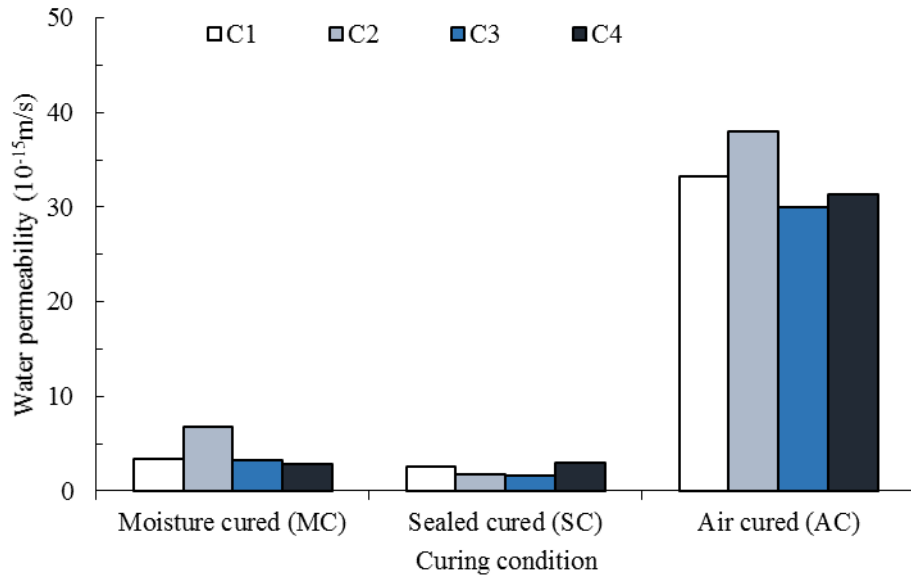


Fig 9-a: Results of water permeability

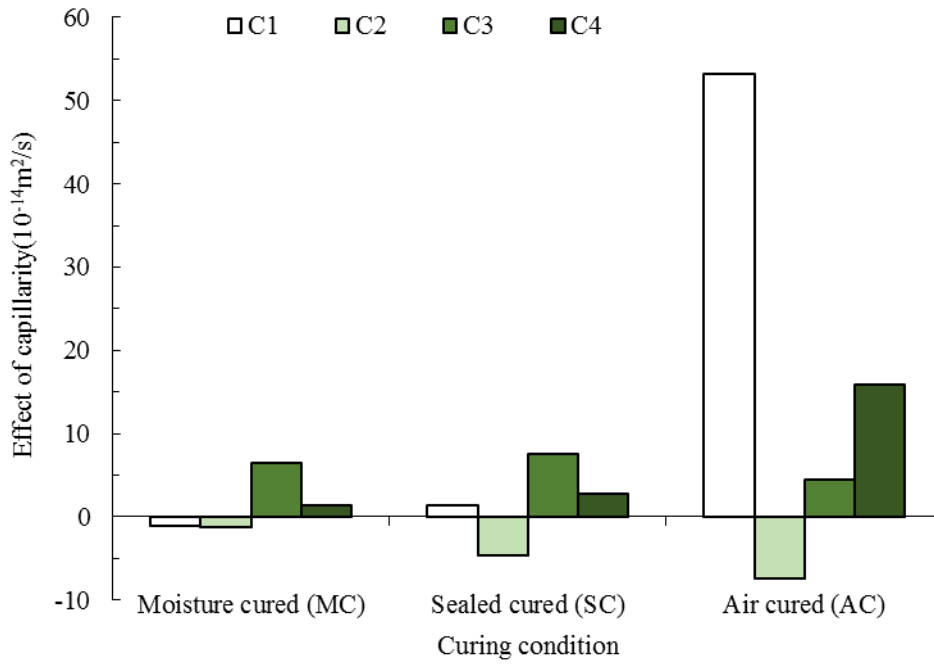


Fig 9-b: Results of effect of capillarity

Note: initial moisture conditions (C1 to C4) are defined in Fig. 2.

Fig. 9 Results of the water permeability and capillarity under different initial moisture conditions

(Note: $1 \text{ m}=39.4 \text{ in.}; 1 \text{ m}^2=1.55 \times 10^3 \text{ in.}^2$)